Research on Engineering Structures & Materials
www.jresm.org
Research Group

Research Article

Coordinated optimal scheduling model for renewable energy generation system based on MBSO algorithm

Jia Lu [*,1,a], Junjie Wang [2,b]

[1]*Department of Electronic Engineering, Taiyuan Institute of Technology, Taiyuan, 030008, China*
[2]*Department of Production and Environmental Protection, China Huaneng Group CO., Ltd. Shandong Branch, Jinan, 250014, China*

Article Info

Article History:

Received 02 Jul 2026

Accepted 19 Sep 2026

Keywords:

Renewable energy generation systems;
Active distribution systems;
Multi-objective brainstorming optimization algorithms;
Optimal scheduling;
Group intelligence

Abstract

With the worsening environmental pollution and increasingly severe problem of resource depletion, an efficient integration and optimized utilization of Renewable Energy (RE) in power generation systems has become a research focus. If RE is to be utilized efficiently, the reliability of power supply and power quality of the distribution system should be improved. However, a basic coordinated optimal scheduling model cannot satisfy the requirement of efficient utilization of RE. To this end, an improved multi-objective brainstorming optimization algorithm is proposed, which enhances the global search capability and convergence accuracy of the algorithm by introducing non dominated sorting and crowding degree computing mechanisms. The experimental results showed that in the testing of three functions (Sphere, Step, and Rastrigin functions), the optimal values of the proposed algorithm (MBSO) were 0.0132, 0.0119, and 0.0657, respectively, with variances of 1.10×10^{-4}, 1.60×10^{-4}, and 6.10×10^{-5}. These results were better than those of the BSO algorithm in terms of optimal value, average value, variance, and standard deviation, demonstrating higher stability and optimization accuracy. In addition, the p-values for the three functions were 0.003, 0.007, and 0.011, respectively, all less than 0.05, indicating that the differences between MBSO and BSO were statistically significant. In the power grid simulation based on actual wind and solar power output data, the optimized system's node voltage prediction error is controlled between 0 and 0.003, and the voltage stability is improved from 0.37 to 0.41. Further results show that the proportion and utilization rate of RE have increased by 1.09% and 11.21%, respectively. The results indicate the effectiveness and feasibility of the proposed method in improving the energy efficiency of the power system and the level of RE access.

© 2026 MIM Research Group. All rights reserved.

1. Introduction

1.1 Motivation and Background of The Study

The use of fossil fuels results in environmental pollution and causes human health issues. The use of Renewable Energy (RE) to generate electricity in the future will help to resolve some of these environmental problems [1-3]. Although the scale of the RE Generation System (REGS) in China is large at present, the utilization rate of RE is not enough to match the system demand. Especially in northwest China, where wind and solar energy resources are abundant, REGS does not efficiently utilize these resources for the conversion and storage of electric energy [4-5]. If RE is to be utilized efficiently, the reliability of power supply and power quality of the distribution system should be improved [6]. Nowadays, REGS has been successfully operated in conjunction with an Active Distribution System (ADS). However, a basic Coordinated Optimal Scheduling Model (COSM) cannot satisfy the current situation of efficient utilization of RE. Therefore, an enhanced COSM is

*Corresponding author: lujia44588@outlook.com
[a]https://orcid.org/0009-0009-2198-9050; [b]https://orcid.org/0009-0005-7770-2849
DOI: http://dx.doi.org/10.17515/resm2026-1814en0702rs

needed to improve the utilization of the distribution system. Brainstorming Optimization (BSO) algorithm can integrate collective learning and individual learning to find an optimal solution. However, the traditional BSO algorithm is prone to premature maturity during the optimization process, and the convergence speed and accuracy performance also need to be improved [7-8].

Based on this background, this study proposes a REGS-based COSM using the multi-objective BSO (MBSO) algorithm. This algorithm innovatively integrates non-dominated sorting and crowding calculation mechanisms into the traditional BSO algorithm to improve the algorithm's global search capability and optimization accuracy. Moreover, a collaborative optimization framework is constructed for REGS and ADS. This framework efficiently utilizes RE and ensures the power grid operates stably by optimizing the operation of controllable units. Compared with existing research, this novel work proposes the deep coupling of the improved MBSO algorithm and REGS for solving the problem of using RE in a smart grid environment.

1.2 Comprehensive Literature Review on The Topic

BSO is a new Group Intelligence (GI) algorithm that simulates the thinking process of the human mind [9-10]. In reference [11], Guo X et al. proposed a new software defect recognition model based on the BSO algorithm. First, the data in the executing software was clustered and sampled using the K-nearest neighbor algorithm. Then, any duplicate data in the sample was removed. Finally, the optimal values of the displacement factor and interlayer connection weights were extracted for training in a wavelet neural network. The results demonstrated that the model was capable of accurately recognizing software defects.

In reference [12], Alwohaibi M et al. concluded that the prediction of breast cancer recurrence probability using machine learning methods can be affected by certain features leading to inaccurate results. Therefore, the BSO algorithm was used for further refinement. The methods were first statistically feature selected for two breast cancer recurrence datasets. Each approach was assessed based on the variant correlation rating, and the BSO algorithm ultimately determined which solution best matched the features. The outcomes showed that the BSO algorithm-incorporated multi-stage learning strategy increased classification accuracy. In reference [13], Lavrič F et al. improved the BSO algorithm and proposed an open AI model. The model then synthesized a collection of concepts from artificial generation and artificial intelligence, embodied in the form of word clouds and images. By comparing the two collections, the correlation between the length and the time required to generate ideas was confirmed. The results proved the feasibility of the model to categorize and set priorities for ideas.

In reference [14], Raamesh L et al. proposed a software fault detection model that incorporates long- and short-term memory and combines late acceptance hill climbing BSO algorithm for improving software reliability. After testing the proposed model through Bugzilla and Firefox datasets, it was confirmed that the proposed model has the advantage of low cost and short execution time. The results indicated that the model effectively improved the defects of the original model which was difficult to integrate. References [15-16] showed that with the increasing complexity of energy systems and the widespread application of distributed energy, the application of optimization algorithms in power system and microgrid management has received widespread attention.

In reference [17], Makahleh F M et al. studied the role, distribution, and power generation of Energy Storage (ES) systems in two-stage power grid peak shaving. The minimum and maximum loads of the ES system network were calculated using Genetic Algorithm (GA) and Particle Swarm Optimization (PSO). The results showed that with the help of peak shaving methods, ES systems could make the load curve of the distribution system to be stable without significant fluctuations, reflecting their economic and technological importance. In reference [18], Habib S et al. proposed an improved bee mating optimization algorithm for economic emission scheduling in power systems. This algorithm improved the local and global search capabilities through adaptive nonlinear systems, and used the final optimization result as a stopping condition. The Simulation Results (SRs) showed that this algorithm was superior to other traditional methods in solving economic load allocation problems.

In reference [19], Kamarposhti M A et al. considered microgrid optimization planning for electricity market capacity to increase resource participation. The study used NSGA-II multi-objective GA to analyze microgrids including solar, wind, microturbines, fuel cells, and batteries, and it designed three scenarios. The introduction of uncertainty through probability distribution functions and the roulette wheel method validated the effectiveness of the proposed algorithm in the three scenarios. In reference [20], Shokouhandeh et al. proposed an improved imperialistic competition algorithm for optimal energy management of microgrids with parking lots and distributed generation units. The study performed 24-hour scheduling of distributed generation units and electric vehicle parking lots under two scenarios and compared the results. SRs showed that this algorithm outperformed GAs and PSO algorithms.

In reference [21], Li et al. proposed a distributed energy rapid recovery optimization strategy based on model predictive control. This strategy achieved short-term global coordination and autonomous regulation. The strategy involved constructing an optimization model that incorporated energy management and critical load recovery through prediction of the power grid's state under abnormal operating conditions. SRs demonstrated that this method significantly enhanced the recovery efficiency and resilience of the distribution network within the IEEE 35 node system. In reference [22], Hiremath R et al. proposed an improved second-order sliding mode controller that enhances the low-voltage ride-through capability using a gain-added hyper-distortion algorithm. This scheme introduced a small amount of positive gain into the switching function, which effectively maintained the voltage margin and DC link stability of the doubly fed fan system. Experiments showed that this method suppressed the chattering phenomenon and improved zero convergence performance while simplifying the coordinate transformation process. In reference [23], Sundarajoo et al. proposed an online monitoring technology for voltage stability in distribution networks that is based on Artificial Neural Networks (ANNs). This method used the local voltage Stability Index (SI) to identify weak busbars, making it more advantageous than traditional load margin methods. The method established a nonlinear mapping relationship between the distribution network control state and the SI by ANN, and combined with the real-time data from the PMU to quickly estimate the SI value. The results demonstrated that this scheme significantly improved the efficiency of SI calculations, enabled real-time voltage stability evaluations, and supported power grid operational decisions.

1.3 Research Gap, Novelty, And Research Objectives

Based on the literature review in Section 1.2, the research gap can be identified as follows. Although many scholars have studied improvements to the BSO algorithm and the development of renewable energy and power generation systems, few studies have combined an improved BSO with a REGS to establish a COSM for an ADS. Moreover, most existing studies on REGS have not quantitatively demonstrated any improvement in Voltage Quality (VQ) and RE utilization.

To fill this gap, this study offers three novel contributions relative to the existing literature. First, unlike the traditional BSO algorithm, which is prone to premature maturity and insufficient convergence accuracy, this study innovatively integrates non-dominated sorting and crowding degree computing mechanisms into the traditional BSO algorithm, enabling the improved MBSO algorithm to handle multiple objectives simultaneously while maintaining the diversity of the Pareto solution set. Second, unlike existing studies that treat the REGS and the ADS separately, this study constructs a collaborative optimization framework that deeply couples REGS with ADS, in which distributed generation, ES units and micro gas turbines are coordinately scheduled subject to constraints on power balance, node voltage, unit output and state of charge. Third, unlike most existing studies that only evaluate the optimization performance on benchmark functions, this study validates the proposed method on actual wind and solar power output data from northwest China and quantitatively demonstrates its advantages in VQ, RE generation ratio, RE utilization ratio and SV.

This study aims to improve the efficiency of REGS in utilizing renewable resources such as wind and photovoltaic power by integrating coordinated scheduling optimization with MBSO, thereby addressing the shortcomings of traditional BSO in convergence performance and optimization accuracy.

The remainder of this paper is organized as follows. Section 2 describes the design of the MBSO algorithm and the COSM for REGS in detail. Section 3 presents the experimental results and discussion. Section 4 concludes the study and outlines the limitations and practical applicability of the proposed method.

2. Cosm Design for Regs Based on MBSO Algorithm

The study firstly updates and improves the BSO algorithm to obtain the MBSO algorithm, builds the COSM of REGS through ADS, and imposes constraints on the controllable units such as distributed power generation and ES devices in the model. Finally, MBSO algorithm is combined with the model to complete the COSM of REGS.

2.1 Studied Data – Description of The Input Data, Sources, And Assumptions

To test the COSM of REGS based on MBSO algorithm, the study utilizes MATLAB software for simulation tests. The simulation is performed on the IEEE 35-node active distribution network shown in Figure 5, where five monitoring nodes (11, 17, 23, 29, and 35) are selected for voltage verification, and the wind and photovoltaic generation data are obtained from an actual wind-solar power station in northwest China with a sampling interval of 15 minutes over a 24-hour horizon (96 scheduling points), while the ES units are configured with a capacity limit of 0.2–0.9 in terms of SOC, a maximum charging and discharging power of 500 kW, and an initial SOC equal to the terminal SOC to satisfy the energy conservation constraint in Eq. (12). The scheduling results at specific moments are verified in conjunction with DIgSILENT simulation software. Using actual wind and solar power generation data from a specific region in northwest China, the data sampling frequency is once every 15 minutes, covering a 24-hour period.

2.2 Considered Algorithm – Detailed Explanation of The Modelling Approach and Simulation Framework

2.2.1 Design of The MBSO Algorithm

The BSO algorithm is a collective thinking method that can quickly search for a solution to a problem. As a kind of GI optimization algorithm, the algorithm has strong global optimization search ability and is widely used in many optimization problems. The scheduling model's optimal solution is sought using the BSO algorithm. The original BSO algorithm follows four rules, namely, quality in quantity, brainstorming (or free thinking), delayed judgment and combined improvement. Among them, quality in quantity requires participants in the discussion to put forward as many ideas as possible to ensure the existence of the best solution. Brainstorming (or free thinking) requires discussants to think out-of-the-box, regardless of whether the ideas are good or bad. Moreover, delayed judgment further guarantees that discussants can express their opinions without burden. Combination improvement can lead people to generate new inspiration from existing ones to find an optimal solution. Based on the above four rules, the BSO algorithm satisfies the rule of quality in quantity to randomly generate the initial population. In the iterative process, group discussion is adopted to determine the better solution within the clusters, and then be further integrated. Several sets of probability parameters are set to regulate the local and global search ability. The optimization process of the BSO algorithm consists of four main components: clustering, mutation, generation of new individuals, and the selection mechanism. In the inter-group discussion phase, the algorithm randomly selects two different groups and pushes potential candidate solutions through these groups. The computational process is shown in Equation (1).

$$X_c = \omega^* X_{c1} + (1-\omega)^* X_{c2} \tag{1}$$

In Equation (1), X_{c1} and X_{c2} denote individuals from two random clusters, respectively. X_c denotes the new individual obtained from fusion. ω denotes the scale adjustment coefficient, $\omega \in (0,1)$. Equation (1) specifies how candidate individuals are generated in the cross-group discussion stage of the MBSO algorithm. Specifically, the decision variables are individuals from two random clusters, which are linearly weighted and fused through the scale adjustment coefficient to obtain new candidate individuals. This equation captures the basic mechanism of

group discussion and information fusion in the BSO algorithm. Its goal is to expand the search range by combining individuals from different clusters and to prevent the algorithm from prematurely converging to local optima. During the generation of new individuals, the probability is randomly perturbed to update the candidate individuals, as shown in Equation (2).

$$\mathrm{X}_n = X_c + \zeta \cdot N(\eta, \sigma) \tag{2}$$

In Equation (2), X_n denotes a newly generated individual. $N(\eta, \sigma)$ denotes the Gaussian random function. Among them, η and σ denote mean and variance, respectively. ζ denotes the perturbation coefficient, and ζ is calculated as in Equation (3).

$$\zeta = \log sig \frac{(0.5 \cdot I_{\max} - I_c)}{k} rand(0,1) \tag{3}$$

In Equation (3), $I_{\max}$ denotes the maximum number of iterations. k denotes the slope. I_c denotes the current iteration number. $rand(0,1)$ denotes the random value between 0 and 1. $\log sig()$ denotes S-type transfer function as shown in Equation (4).

$$\log sig(a) = \frac{1}{1+e^{-a}} \tag{4}$$

In Equation (4), a denotes the variable substituted into the $\log sig()$ function. e^{-a} denotes the base of $\log sig()$. Equation (2) describes the operation of applying random perturbations to candidate individuals during the generation of new individuals. This equation enables a neighborhood search around the existing candidate solutions, thereby enhancing the local development capability of the algorithm and providing a source of diversity for selecting better individuals in the subsequent steps. Equation (3) provides the calculation method for the perturbation coefficient. This equation dynamically adjusts the perturbation intensity through a logarithmic function, allowing the algorithm to have a larger search step size in the early iterations and gradually reduce the perturbation in the later iterations, thus balancing global search and local convergence. Equation (4) defines the function of Equation (3), which functions to perform smooth nonlinear regulation of the iterative process, causing the perturbation coefficient to gradually change with the iterative progress. A comparison is made between the recently created individual X_n and the one that is now formed. To get closer to the global optimal solution, the better term is chosen. The advantage of the BSO algorithm is the clustering selection. The individual update method is shown in Figure 1.

Figure 1(a) is the process of cross-group optimization search. The clustering centers of the two groups are computed and searched globally to obtain candidate individuals, and early results are obtained. Figure 1(b) is the process of determining the clustering center within a group. The algorithm will randomly determine a clustering center as a candidate solution, narrowing the search focus to a region close to the optimal solution, thus accelerating the convergence process of the algorithm.

The ratio of global search to local search can be effectively regulated by these two grouping methods. However, due to the effect of random probability in the BSO algorithm, the learning process of the clustering center is unstable, and the overall efficiency of the optimization search is slow. Therefore, the study proposes a model using MBSO to improve the updating method to achieve the optimization of the objectives. MBSO achieves efficient optimization by improving the coordination between multiple objectives and considering the establishment angle of each objective. MBSO seeks the maximum problem as shown in Equation (5).

$$obj.\max F(x) = (f_1(x), f_2(x), \ldots, f_m(x))^T \tag{5}$$

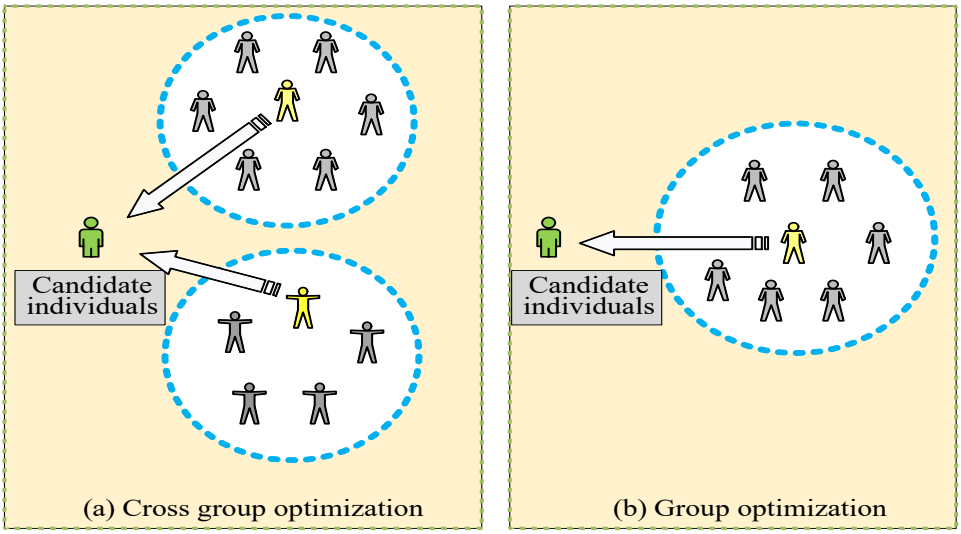

Fig. 1. Schematic diagram of individual update methods

In Equation (5), x denotes the n-dimensional control variable. $x \in R^n$ and $F(x)$ denote the m-dimensional objective space. Equation (5) presents the mathematical form of the multi-objective optimization problem solved by the MBSO algorithm. This equation clearly indicates that MBSO deals with multi-objective maximization problems, where multiple objective functions are simultaneously optimized, rather than simply aggregating them into a single objective. The mathematical objective function of the model specifically includes VQ targets, targets for the proportion of RE generation, targets for the utilization rate of RE, and satisfaction targets. Specifically, as shown in Equation (6).

$$\begin{aligned}
&\min f_1 = \sum_{t=1}^{T}\sum_{a=1}^{A}(U_{a,t} - U_A)^2 \\
&\max f_2 = \frac{\sum_{t=1}^{T}(\mathbf{P}_t^{\text{wind}} + \mathbf{P}_t^{\text{pv}})}{\sum_{t=1}^{T}\mathbf{P}_t^{\text{total}}} \times 100\% \\
&\max f_3 = \left(1 - \frac{\sum_{t=1}^{T}(\mathbf{P}_t^{\text{cur,wind}} + \mathbf{P}_t^{\text{cur,pv}})}{\sum_{t=1}^{T}(\mathbf{P}_t^{\text{wind,max}} + \mathbf{P}_t^{\text{pv,max}})}\right) \times 100\% \\
&\max f_4 = \zeta_1 \cdot \xi_{\text{VQ}} + \zeta_2 \cdot \xi_{\text{rel}} + \zeta_3 \cdot \xi_{\text{acc}}, \sum_b \zeta_b = 1
\end{aligned} \tag{6}$$

In Equation (6), f_1 is the VQ objective function; t is the time period number; T is the total number of time periods within the scheduling cycle; a is the node number; A is the total number of system nodes; $U_{a,t}$ is the voltage per-unit value of node a in time period t; U_A is the rated voltage per-unit value; f_2 is the target proportion of RE generation; $\mathbf{P}_t^{\text{wind}}$ is the actual output of wind power in time period t; $\mathbf{P}_t^{\text{pv}}$ is the actual output of photovoltaic power in time period t; $\mathbf{P}_t^{\text{cur,wind}}$ is the total power generation of the system in time period t; $\mathbf{P}_t^{\text{cur,wind}}$ is the curtailed wind power in time period t; $\mathbf{P}_t^{\text{cur,pv}}$ is the curtailed photovoltaic power in time period t; $\mathbf{P}_t^{\text{wind,max}}$ is the maximum allowable power output of wind power in time period t; $\mathbf{P}_t^{\text{pv,max}}$ is the maximum allowable power output of photovoltaic power in time period t. $F(x) \in R^m$ and $f(x)$ denote the objective function. The constraint equations are shown in Equation (7).

$$s.t.\begin{cases} h_i(x)=0, i=1,2,...,p \\ g_j(x)\le 0, j=1,2,...,q \end{cases} \tag{7}$$

In Equation (7), $h_i(x)=0, i=1,2,...,p$ denotes p equality constraint. $g_j(x)=0, j=1,2,...,q$ denotes q constraint inequalities. Equation (7) provides the constraints for the multi-objective optimization problem. This formula indicates that during the solution process of the MBSO algorithm, the decision variables must simultaneously satisfy both equality and inequality constraints. These constraints jointly define the feasible solution space and form the basis for subsequent non-dominated sorting and crowding degree calculation. Let the two solutions in the space be M and N, and the expression is shown in Equation (8).

$$\begin{cases} f_i(M)\ge f_i(N), \forall i\in(1,2,...,m) \\ f_j(M)\ge f_j(N), \exists j\in(1,2,...,m) \end{cases} \tag{8}$$

In Equation (8), if M and N satisfy the above equation, M is a non-dominated solution and N is a dominated solution. If it is not satisfied, M is the optimal solution set of $F(x)$. Equation (8) provides the criteria for determining non-dominated and dominated solutions in multi-objective optimization. It is the core basis for introducing the non-dominated sorting mechanism in the MBSO algorithm. It serves to evaluate the superiority and inferiority relationships among multiple objectives and to construct the Pareto optimal solution set. The clustering process of the MBSO algorithm is a convergent operation, which mainly creates conditions for the subsequent update iterations of the selection and mutation operations, as shown in Figure 2.

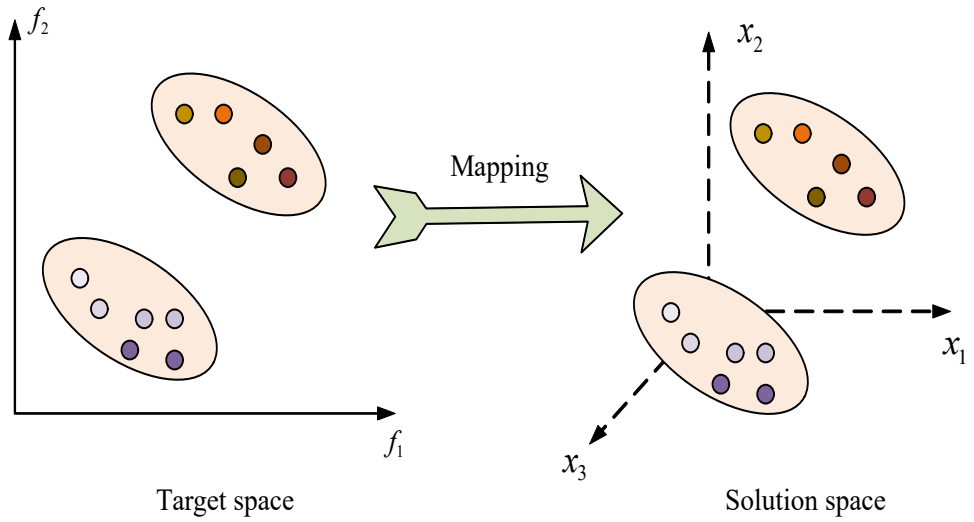

Fig. 2. Clustering in the target space

In Figure 2, C_1 in the target space denotes the elite class. C_2 denotes the ordinary class, corresponding to S_1 and S_2 in the solution space, respectively. S_1 denotes the elite solution set. S_2 denotes the ordinary solution set. The MBSO algorithm overcomes the limitation of other GI optimization algorithms that rely only on individual positions in global optimization search through the mechanism of individual clustering. The selection operation is mainly based on different rules to select the variant operating individuals, as shown in Figure 3.

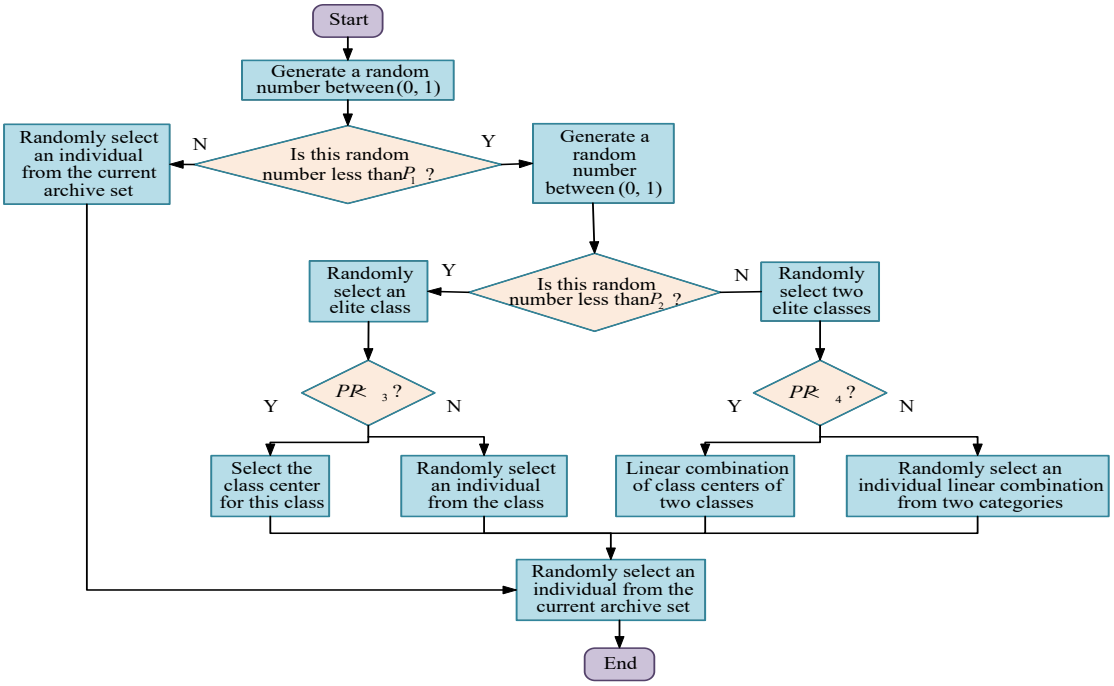

Fig. 3. The selection process of BSO

In Figure 3, P_1, P_2, P_3, and P_4 denote four different probability values. P_1 determines whether to select individuals from the current archive pool for further processing or optimization. P_2 denotes the number of selected clusters. The main role of P_3 and P_4 is to determine the variant initial value. While the variation operation is to search the neighborhood of the selected individuals, the study uses Gaussian variation to help generate new individuals. Finally, the algorithm updates the non-dominated solutions obtained in the iteration and saves them in the archive set. If the number of solutions in the archive set exceeds the predefined capacity, the degree of crowding of each solution needs to be evaluated. Based on this, a distance calculation is performed to exclude the solution with the smallest result and then proceed to the next round of iteration.

2.2.2 COSM for REGS Based on MBSO Algorithm

The study builds a COSM for REGS through ADS in an attempt to realize the efficient utilization of RE. The model needs to consider several controllable units in the ADS, such as distributed generation, ES units, etc. The ADS structure is shown in Figure 4.

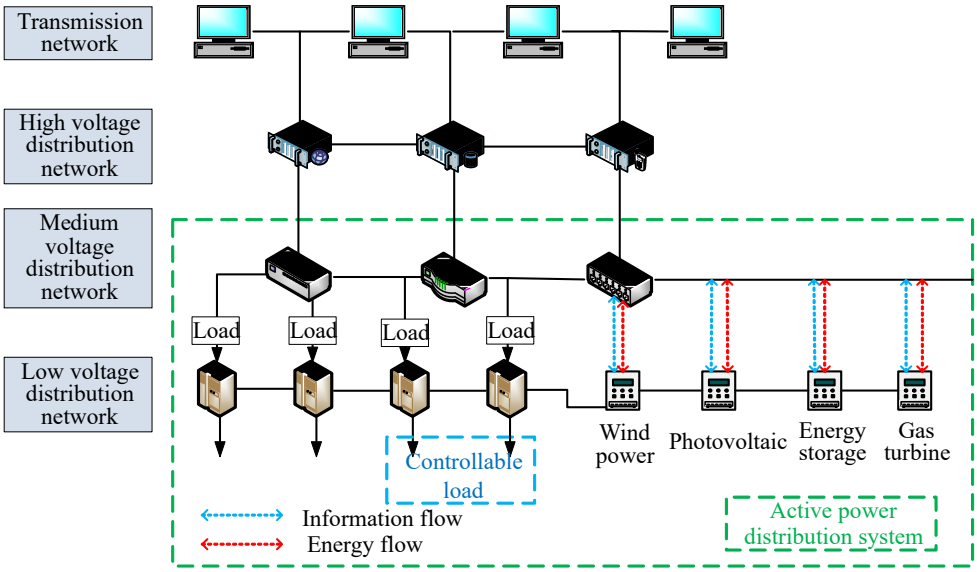

Fig. 4. Structural diagram of active power distribution system

In Figure 4, there are a wide variety of distributed generation units, including wind power, photovoltaic, and micro gas turbine power generation and other distributed generation. Among them, renewable distributed generation can efficiently utilize renewable clean energy and is an important auxiliary power generation part of ADS. Micro gas turbine has the advantages of smooth power output and fast response speed. Moreover, the ES unit can quickly adjust the charging power and other conditions to adapt to the system scheduling demand and reduce the load during the peak power consumption. On this basis, the study mainly optimizes the system VQ and the efficient use of RE. Considering the relationship between the variables in the mathematical model, constraints need to be imposed on the controllable units. The power balance constraints are shown in Equation (9).

$$P_i = U_i \sum_{j \in i} U_j (G_{ij} \cos\theta_{ij} + B_{ij} \sin\theta_{ij}) \tag{9}$$

In Equation (9), i and j denote the injection nodes. P_i is the active power of i. G_{ij} and B_{ij} together denote the node conductance matrix. U_i and U_j represent the voltage magnitude of i and j, respectively. Equation (9) provides the active power balance constraints in the active distribution network. The equation indicates that the active power at each node of the system must satisfy the network power flow relationship, which is an important constraint for determining whether the power balance is satisfied in the coordinated optimization scheduling model. The node voltage constraints are shown in Equation (10).

$$Q_i = U_i \sum_{j \in i} U_j (G_{ij} \sin\theta_{ij} - B_{ij} \cos\theta_{ij}) \tag{10}$$

In Equation (10), Q_i denotes the reactive power of i. U_i takes the value of $U_i^{\min} \le U_i \le U_i^{\max}$. $U_i^{\min}$ and $U_i^{\max}$ represent the upper and lower limits (ULL) of voltage magnitude respectively. Equation (10) provides the reactive power balance constraints in the active distribution network. This equation serves to describe the distribution relationship of reactive power among nodes. Moreover, in combination with the voltage amplitude constraints, ensures that the system voltage operates within the allowable range. The active and reactive power output constraints of each distributed generation unit are shown in Equation (11).

$$\begin{cases} \mathrm{P}_r^{\min} \le P_r(t) \le P_r^{\max} \\ Q_r^{\min} \le Q_r(t) \le Q_r^{\max} \end{cases} \tag{11}$$

In Equation (11), P_r denotes the active power output from the r th renewable distributed generation unit. t denotes the moment. $Q_r(t)$ denotes the reactive power. $\mathrm{P}_r^{\min}$ and $\mathrm{P}_r^{\max}$ denote the ULL of active output power, respectively. $Q_r^{\min}$ and $Q_r^{\max}$ denote the ULL of the active output, respectively, $(Q_r^{\max}, Q_r^{\min}) = f\left[P_r(t)\right]$. Equation (11) provides the constraints on the active and reactive power output of each distributed generation unit. This constraint indicates that the output of the distributed generation units cannot be arbitrarily set, but must remain within the specified power range to ensure system safety and stability. Equation (12) illustrates the ES device's state of charge (SOC) restrictions.

$$SOC_j^{\min} \le SOC_j(t) \le SOC_j^{\max} \tag{12}$$

In Equation (12), $SOC_j^{\max}$ and $SOC_j^{\min}$ denote the ULL of the capacity of j ES devices, respectively. j denotes the number of ES devices. Equation (12) specifies the charge state constraint for the ES device, which limits the energy state of the ES equipment during the charging

and discharging process, thereby preventing overcharging or over discharging, extending the lifespan of the ES device, and ensuring the feasibility of the scheduling plan. The expression of the energy conservation constraint at the end of the dispatch cycle is shown in Equation (13).

$$SOC_j(0) = SOC_j(k\Delta t) \tag{13}$$

In Equation (13), $SOC_j(0)$ denotes the initial energy. $SOC_j(k\Delta t)$ denotes the residual energy. Equation (13) presents the energy conservation constraint at the end of the scheduling period. This equation requires the ES device to return to its initial energy state after each complete scheduling period, thereby ensuring energy balance and sustainable operation across successive scheduling periods. The constraint expressions for charging and discharging states and power are shown in Equation (14).

$$\begin{cases} P_{Ej}^{c}(t)P_{Ej}^{d}(t) = 0 \\ P_{Ej}^{c.\max} \le P_{Ej}^{c}(t) \le 0 \\ 0 \le P_{Ej}^{d}(t) \le P_{Ej}^{d.\max} \end{cases} \tag{14}$$

In Equation (14), $P_{Ej}^{c}(t)$ denotes the charging power output from the j th ES device at the t moment. $P_{Ej}^{d}(t)$ discharge power. $P_{Ej}^{c.\max}$ and $P_{Ej}^{d.\max}$ denote the upper limits of charging and discharging powers respectively. Equation (14) provides the charging and discharging status as well as power constraints for the ES device. This equation ensures that the ES device cannot be both charging and discharging, and imposes upper and lower limits on the charging and discharging power. It is an important constraint condition for the ES scheduling decision. The ADS arithmetic example is schematically shown in Figure 5.

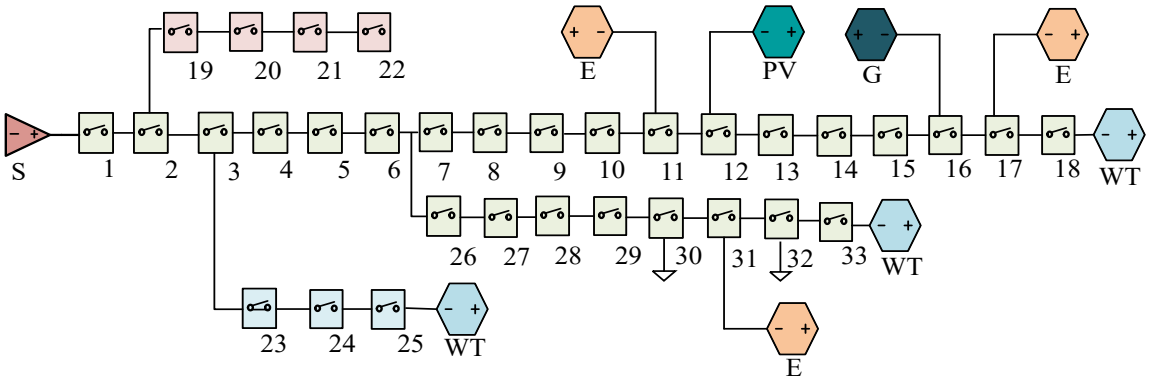

Fig. 5. Schematic diagram of active power distribution system

Figure 5 is an example of the calculation process of ADS. A COSM for REGS based on MBSO algorithm is obtained by combining MBSO algorithm with optimal scheduling model. The process is shown in Figure 6.

In Figure 6, first, the parameters of the ADS, each controllable component, and the MBSO algorithm, such as the initial individual and the maximum iterations, need to be collected and configured. N uniformly distributed individuals are generated after the parameters are set. Subsequently, the objective function values of each solution vector are computed in parallel and non-dominated sorting is performed to establish a hierarchical relationship of solutions and quantitatively evaluate their quality. After storing in the archive set, the initial scheduling vectors are in the two-dimensional objective space using the maximum correlation entropy criterion. Based on the analysis and grouping of the non-dominated ranking, the class of solutions is classified as standard and excellent. Specifically, the level of solutions is evaluated based on the relative superiority of different solutions in the target space. Then new individuals are generated based on selection and mutation operations, as shown in Equation (15).

$$x_{new}^{d} = x_{selected}^{d} + \xi \cdot N(\mu, \sigma) \tag{15}$$

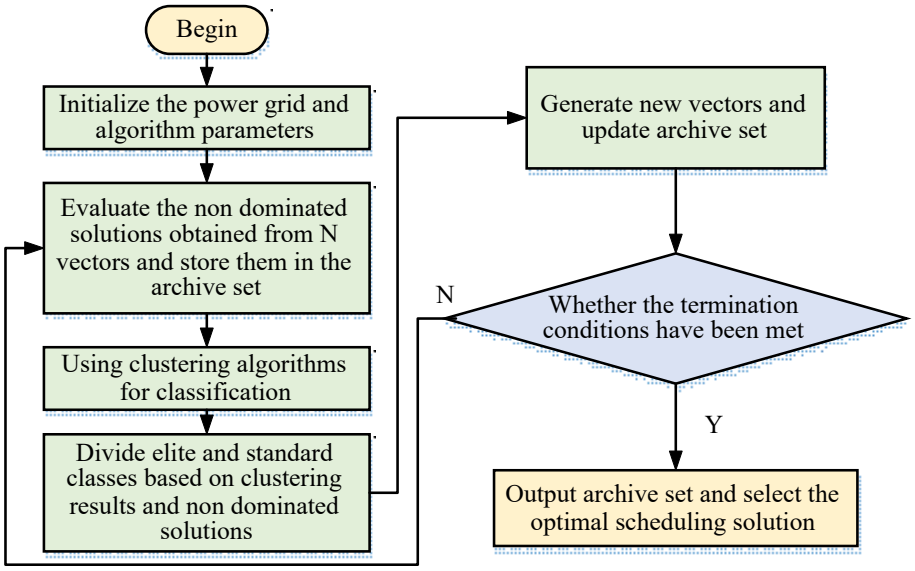

Fig. 6. Distribution system flowchart using MBSO

In Equation (15), x_{new}^{d} denotes the power value of dimension d in the new vector. $x_{selected}^{d}$ denotes the power value of dimension d of the vector being updated. μ denotes the mean value. σ denotes the variance. $N(\mu, \sigma)$ denotes the Gaussian random function. ξ denotes the value of the weight coefficient in generating the new scheduling. Equation (15) presents the method by which the MBSO algorithm generates new scheduling vectors in the collaborative optimization scheduling model. Specifically, the decision variables are the power values of each controllable unit during the collaborative optimization scheduling process. New individuals are generated by applying Gaussian mutation to selected individuals, thereby enabling iterative updates of the scheduling plan and the search for Pareto optimal solutions. The non-dominated solutions are compared with each solution vector in the archive set. After checking, if there are more scheduling vectors in the archive set than there is space for, calculate the congestion gap between each vector and eliminate any invalid ones. This process is repeated until the optimal solution is identified or the specified condition is met. At this point, the program is terminated and the Pareto solution set is outputted as the archive set.

To quantitatively evaluate the effectiveness of the proposed COSM in REGS, the following four performance indicators are defined:

- VQ. It is defined as the degree of closeness between the voltage at the active distribution network nodes and the rated voltage after optimization scheduling. The higher the VQ value, the smaller the deviation of the node voltage from the rated value, indicating better voltage stability of the system.
- Satisfaction Value (SV). SV is defined as the degree to which the scheduling plan meets the operational requirements of the system, comprehensively reflecting the voltage qualification rate, power supply reliability, and the acceptance capacity of RE. The higher the SV, the more the scheduling plan can meet the operational needs of the system and users.
- Renewable Energy Generation Ratio (REGR). It is defined as the proportion of RE generation (including wind energy and photovoltaic power) in the total power generation of the active distribution network. A higher REGR indicates a greater proportion of clean energy in the power supply structure.
- Renewable Energy Generation Utilization Efficiency (REUR). It is defined as the proportion of the actual consumption of renewable energy in the total RE. A higher REUR means less RE is curtailed and the utilization efficiency of RE is higher.

These four indicators will serve as the evaluation criteria for comparing the scheduling performance of COSM based on BSO and MBSO.

2.3 Statistical Analysis – Presentation of The Statistical Metrics Used to Evaluate the Results

The study compares the MBSO and BSO algorithms by setting the experimental parameters and selecting three functions, (Sphere, Step and Rastrigin functions), for testing with the NSL-KDD dataset. Then, for performance testing, the MBSO algorithm is compared with the GA and the PSO algorithms [24-25]. Finally, the scheduling results at specific moments, the node voltages before and after optimization, and the results of REGS model based on BSO and MBSO are verified and analyzed for application on DIgSILENT simulation software.

To ensure the reproducibility of the proposed MBSO algorithm, the implementation details, parameter settings, and constraint management procedures are fully described below. The MBSO algorithm is implemented in MATLAB (R2021a) on a computer with an Intel Core i7-10700 CPU at 2.90 GHz and 16 GB RAM. The population size is set to 30, and the maximum number of function evaluations is fixed at 30,000 for all test functions. The dimension of each test function is set to 30. The number of independent runs is 30 for each algorithm on each function. The main control parameters of MBSO include the clan number, set to 5; the maximum number of iterations per clan, set to 20; the probability of selecting the best individual within a clan for generating new solutions, which is set to 0.8. In addition, the mutation probability is set to 0.05, and the step-size scaling factor is set to 0.5. These parameters are determined based on preliminary experiments and kept identical across all test functions to ensure a fair comparison. Regarding constraint management, since the three benchmark functions (Sphere, Step, and Rastrigin) are unconstrained optimization problems, no explicit constraint-handling mechanism is required. However, for potential constrained optimization problems, MBSO adopts a feasibility-rule-based constraint management procedure: when comparing two candidate solutions, a feasible solution is always preferred over an infeasible one; if both solutions are feasible, the one with the better objective function value is selected; if both are infeasible, the one with the smaller total constraint violation is selected. The total constraint violation is calculated as the sum of the violations of all constraints, where each violation is defined as the maximum of zero and the difference between the constraint value and its boundary. This constraint management procedure is integrated into the selection step of MBSO to ensure that the search process is guided toward feasible regions while maintaining population diversity. All these settings and procedures are kept consistent across all experiments to guarantee that the reported results are complete and reproducible.

The study conducts two sets of experiments to evaluate the performance of the proposed MBSO algorithm. The first set employs three standard benchmark functions, namely Sphere, Step and Rastrigin, to verify the convergence accuracy and stability of the algorithm in continuous optimization problems. The second set uses the NSL-KDD dataset, a widely used benchmark for machine learning research on network intrusion detection, to verify the iterative performance of the algorithm in a classification task. These two sets of experiments are independent of each other and serve different evaluation purposes. The training set and test set mentioned in the study refer only to the division of the NSL-KDD dataset, and do not involve the three benchmark functions. The three benchmark functions are used only for convergence testing and are not divided into training and test sets. The NSL-KDD dataset is split into a training set and a test set in a ratio of 6:4, where the training set is used to train the classification model and the test set is used to evaluate evaluate the algorithm's generalization performance on unseen data. The convergence results of the tests are shown in Figure 7.

Figures 7 (a), (b), and (c) represent the optimization curves of MBSO and BSO algorithms on three different types of functions, i.e. Sphere, Step and Rastrigi functions, respectively. In Figure 7 (a), the convergence speed of MBSO algorithm is significantly faster than that of BSO algorithm. The fitness value of MBSO algorithm decreases rapidly in the first 20 iterations and remains stable after that, while the fitness value of BSO algorithm decreases slowly and shows significant fluctuations during the iteration process. This indicates that the MBSO algorithm has a higher optimization accuracy and stability when dealing with Sphere functions. In Figure 7 (b), the MBSO algorithm also exhibits

faster convergence speed and higher optimization accuracy, while the fitness curve of BSO still decreases slowly. In Figure 7 (c), the BSO algorithm exhibits significant fluctuations, slow convergence speed, and low optimization accuracy during the optimization process. MBSO algorithm can converge quickly and remains stable after the 20th iteration. Table 1 displays the MBSO and BSO test results for the three sets of functions.

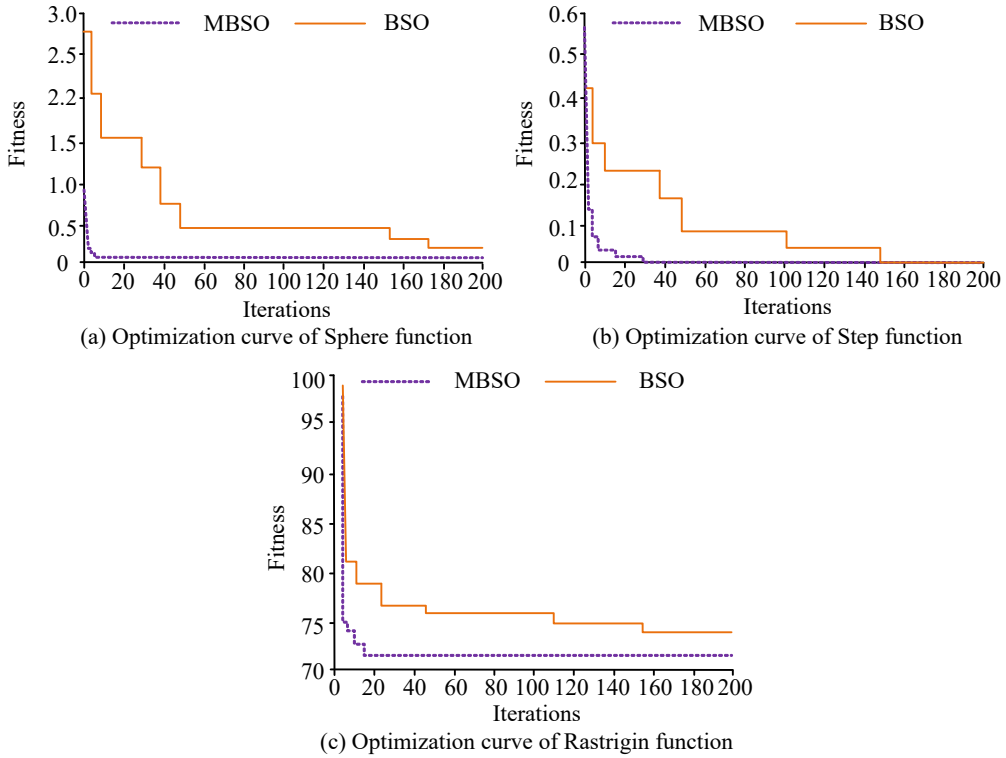

Fig. 7. Optimization curves for three types of functions

Table 1. Test results of two algorithms (BSO, MBSO) on three functions (Sphere, Step and Rastrigin)

Function	Algorithm	Worst value	Optimal value	Average value	Variance	Std. deviation	p-value
Sphere	BSO	0.0934	0.0132	0.0243	3.60×10-4	0.0190	0.003
	MBSO	0.0554	0.0132	0.0198	1.10×10-4	0.0105	
Step	BSO	0.0621	0.0247	0.0396	2.56×10-4	0.0160	0.007
	MBSO	0.0578	0.0119	0.0252	1.60×10-4	0.0126	
Rastrigin	BSO	0.1267	0.0842	0.1053	1.46×10-4	0.0121	0.011
	MBSO	0.0894	0.0657	0.0762	6.10×10-5	0.0078	

Note: All the statistical figures in the table are based on the results of 30 independent runs; Mean and Variance represent the average and variance of the 30 independent runs; p-value is the result of the Wilcoxon rank sum test between MBSO and BSO at a 5% significance level.

According to Table 1, for the Sphere function, MBSO achieves a worst value of 0.0554, lower than BSO's 0.0934; an average value of 0.0198, lower than BSO's 0.0243; a variance of 1.10×10^{-4}, lower than BSO's 3.60×10^{-4}; and a standard deviation of 0.0105, also lower than BSO's 0.0190. This suggests that the overall performance of MBSO is more stable across multiple runs. Moreover, the *p*-value between MBSO and BSO is 0.003 (< 0.05), indicating that the differences between the two algorithms on the Sphere function are statistically significant. On the Step function, MBSO also outperforms BSO. MBSO achieves an optimal value of 0.0119, significantly better than BSO's 0.0247; a worst value of 0.0578, slightly lower than BSO's 0.0621; an average value of 0.0252, lower than BSO's 0.0396; a variance of 1.60×10^{-4}, lower than BSO's 2.56×10^{-4}; and a standard deviation of 0.0126, also lower than BSO's 0.0160. The *p*-value is 0.007 (< 0.05), indicating that MBSO yields significantly better optimization results than BSO on the Step function. For the Rastrigin function,

MBSO attains an optimal value of 0.0657, superior to BSO's 0.0842; a worst value of 0.0894, lower than BSO's 0.1267; an average value of 0.0762, lower than BSO's 0.1053; a variance of 6.10×10^{-5}, lower than BSO's 1.46×10^{-4}; and a standard deviation of 0.0078, also lower than BSO's 0.0121. The *p*-value is 0.011, which is less than 0.05, indicating that MBSO can maintain high optimization accuracy and stability when dealing with this complex nonlinear optimization problem, and the difference between the two algorithms is statistically significant. In conclusion, the worst value, optimal value, average value, variance and standard deviation of the MBSO algorithm on the Sphere, Step and Rastrigin functions are all superior to those of the BSO algorithm, and the *p*-values are all less than 0.05, indicating that MBSO has significant advantages in optimization accuracy, convergence speed and stability. To verify the individual contribution of the two modified components in MBSO, namely the non-dominated sorting mechanism and the crowding degree computing mechanism, an ablation analysis is conducted by constructing three variants of the algorithm: (1) BSO, which is the original algorithm without any modification; (2) MBSO-NS, which only introduces the non-dominated sorting mechanism into BSO; and (3) MBSO, which integrates both non-dominated sorting and crowding degree computing mechanisms. All variants are tested on the Sphere, Step and Rastrigin functions under the same population size, maximum number of iterations, stopping criterion and 30 independent runs, and the results are shown in Table 2.

Table 2. Ablation analysis of the modified components in MBSO

Function	Algorithm	Mean±Variance	Optimal value	Std. deviation
Sphere	BSO	0.0243±0.0338	0.0132	0.1838
Sphere	MBSO-NS	0.0221±0.0247	0.0132	0.1572
Sphere	MBSO	0.0276±0.0183	0.0132	0.1353
Step	BSO	0.0167±0.0393	0.0247	0.1982
Step	MBSO-NS	0.0154±0.0268	0.0183	0.1637
Step	MBSO	0.0185±0.0164	0.0119	0.1281
Rastrigin	BSO	0.0456±0.0256	0.0268	0.1600
Rastrigin	MBSO-NS	0.0412±0.0195	0.0351	0.1396
Rastrigin	MBSO	0.0644±0.0143	0.0657	0.1196

As shown in Table 2, introducing the non-dominated sorting mechanism alone (MBSO-NS) already reduces the variance and standard deviation compared with the original BSO on all three functions, indicating that non-dominated sorting improves the stability of the algorithm by establishing a hierarchical relationship among solutions. When the crowding degree computing mechanism is further added (MBSO), the variance and standard deviation are reduced even more significantly, and the optimal values on the Step and Rastrigin functions improved markedly, which confirms that the crowding degree mechanism plays a key role in maintaining the diversity of the archive set and preventing the algorithm from converging to a narrow region of the Pareto front. The ablation results therefore demonstrate that both modified components contribute individually to the performance improvement of MBSO, and that their combination yields the best overall stability and optimization accuracy.

The improved MBSO algorithm effectively overcomes the limitations of slow convergence speed and low optimization accuracy of traditional BSO. The MBSO algorithm's iterative performance tests are compared with those of BSO, PSO, and GA in an attempt to confirm its effectiveness. The results are shown in Figure 8.

Figures 8(a) and 8(b) represent the iterative performance test results in the training and test set, respectively. In Figure 8(a), the fitness function value of the MBSO algorithm decreases rapidly and reaches 0.2 in the early iterations, maintaining stability and demonstrating a fast convergence speed. In contrast, the convergence speed of the BSO, PSO, and GA is slower and the fitness function value decreases more smoothly during the iteration process. This indicates that the MBSO algorithm has higher optimization accuracy and better stability on the training set. In Figure 8(b), the MBSO algorithm also shows superior performance. The fitness function value decreases rapidly at the beginning of the test and reaches 0.1 at the 80th iteration. Compared to the other three

algorithms, the MBSO algorithm also has high optimization accuracy and stability on the test set, and can effectively transfer the performance on the training set to unseen data.

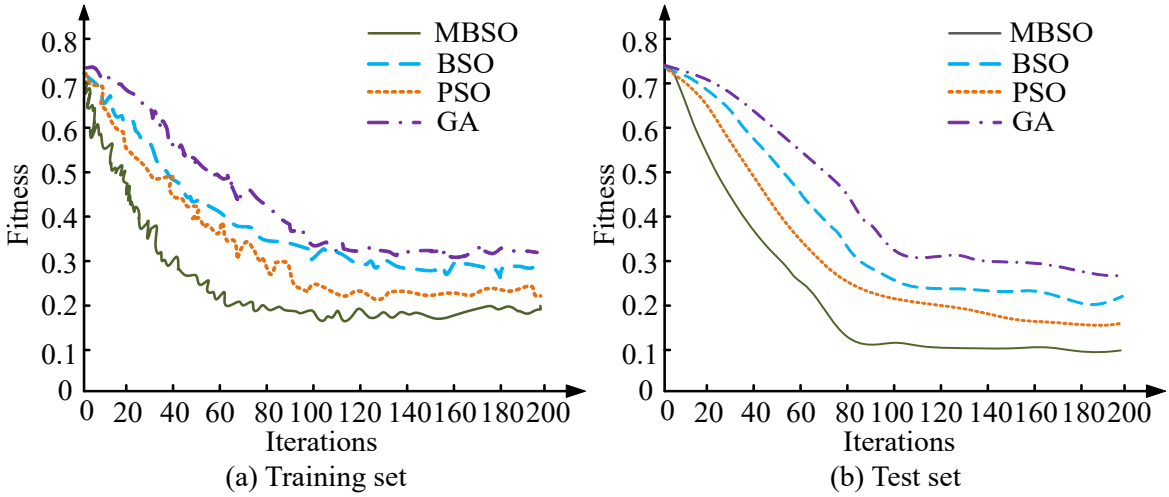

(a) Training set (b) Test set

Fig. 8. Iterative performance testing of four optimization algorithms

2.4 Validation – Model Validation Against Experimental Data, Literature, or Benchmark Cases

The correctness of the scheduling results is verified by selecting five node voltages (11, 17, 23, 29 and 35) at three moments: 1:30, 9:30, and 17:30 hours. The results are shown in Table 3 where the Simulated Results (SRs) can be compared with the Predicted Results (PRs) of the algorithm. In addition, the DIgSILENT simulation is performed under the same 24-hour time horizon and 15-minute resolution as the MATLAB optimization, the load demand is set according to the typical daily load curve of the selected region, the micro gas turbine is modeled with a rated active power of 200 kW and a fast response time of less than 1 minute, and all the above network, renewable generation, storage and algorithm parameter values are summarized to ensure that the proposed COSM for REGS based on MBSO can be fully reproduced.

Table 3. Comparison of simulation and predicted results

Node number	1:30 hrs.			9:30 hrs.			17:30 hrs.		
	SR	PR	Error	SR	PR	Error	SR	PR	Error
11	1.031	1.032	0.001	1.012	1.011	0.001	0.967	0.965	0.002
17	1.023	1.021	0.002	1.052	1.055	0.003	0.987	0.989	0.002
23	0.894	0.896	0.002	0.996	0.996	0.000	0.966	0.967	0.001
29	1.012	1.014	0.002	1.006	1.005	0.001	0.974	0.972	0.002
35	1.025	1.023	0.002	1.016	1.014	0.002	0.988	0.989	0.001

In Table 3, SR is the voltage result obtained by the DIgSILENT simulation software, while PR is the voltage result calculated by the algorithm. The voltage values of the simulated nodes are roughly consistent with those obtained by the program calculations. The error range is within 0 to 0.003, which confirms the accuracy of the program solution results. At 1:30 hrs, the voltage SRs of all nodes are very close to the algorithm calculation results, with errors ranging from 0.001 to 0.002. Except for Node 11, which has an error of 0.001, the errors of all other nodes are 0.002, indicating that the algorithm has high accuracy during low load periods at night. At 9:30 hrs, the errors of most nodes remain in the range of 0.001 to 0.003, but the errors of Nodes 17 and 35 are relatively large, at 0.003 and 0.002, respectively. This may be related to the rapid changes in network load during the morning hours, and the algorithm may have some delay in responding to such changes. At 17:30 hrs, the agreement between the voltage SRs and the algorithm calculation results is still high, with errors ranging from 0.001 to 0.002. This indicates that the algorithm can accurately predict the node voltage in the evening, even under high load conditions. The results comparing the unoptimized scheduling and the optimized scheduling are shown in Figure 9.

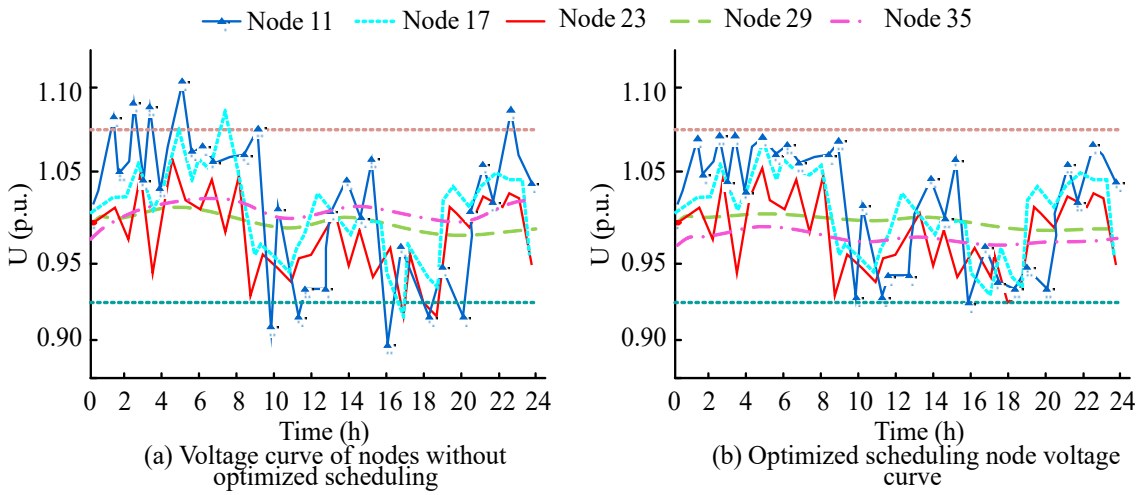

Fig. 9. Unoptimized scheduling and optimized scheduling results

Figure 9(a) is the node voltage profile without optimal dispatch. Due to the high active power generated by wind power generation, the voltage values at Node 11 and Node 17 exceed the maximum national standard of 1.07 p.u. during the time period from 1:00 hrs to 10:00 hrs. Around 17:00 to 21:00 hrs, the active output of wind power and PV is insufficient under high system load. At this time, the voltage values at all five monitoring points drop and are below the national minimum voltage standard. The substandard voltage levels may have a significant impact on power security. Figure 9(b) is the node voltage profile after optimized scheduling. The node voltage is between 0.93 p.u. and 1.07 p.u. at all times. Around 1:00 to 6:00 hrs, the ES unit is in charging state and the wind turbine consumes reactive power during operation. The voltage at each node of the system is gradually reduced and the wind power resources are efficiently utilized. Through the cooperation of the controllable units, between 17:00 and 21:00 hrs, the ES unit starts to discharge and the wind turbine outputs reactive power. To maintain the system's regular operation at this point, the micro gas turbine helps to control the active output and lowers the amount of demand through the curtailment limitation.

The comparative results of the four effectiveness indexes of the improved algorithm are shown in Figure 10. The four effectiveness indexes are: 1) VQ, 2) SV, 3) RE generation ratio, and 4) RE generation utilization ratio.

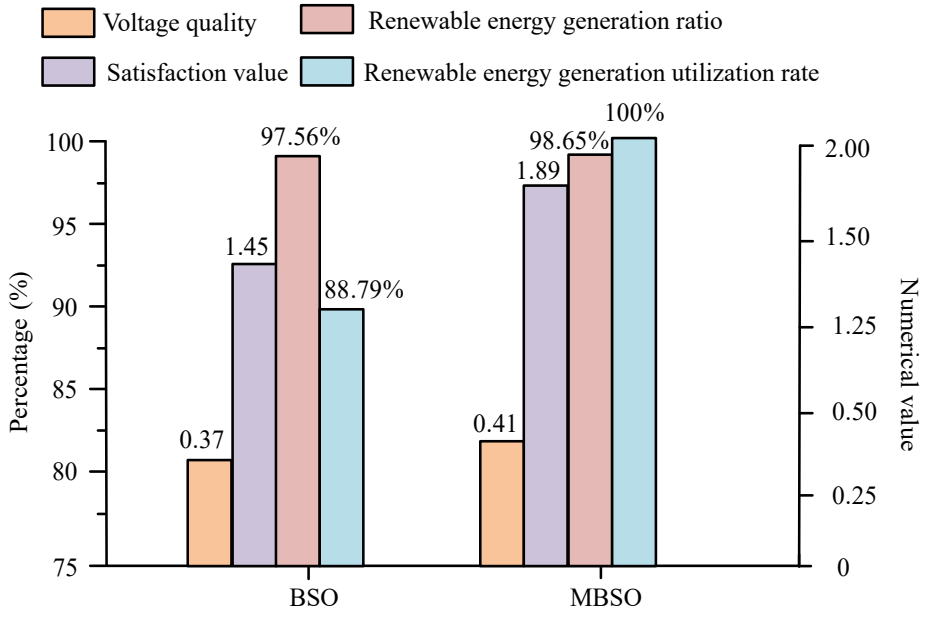

Fig. 10. Comparison of algorithm improvement indicators

Figure 10 shows that the MBSO algorithm outperforms the BSO algorithm in all four effectiveness indexes or metrics. In terms of VQ, the MBSO algorithm scores 0.41, significantly higher than the 0.37 score of the BSO algorithm. This indicates that the BSO algorithm struggles to optimize VQ in power systems and achieve an optimal voltage configuration. The MBSO algorithm can more effectively optimize the VQ of the power system, bringing it closer to the ideal state. In terms of the proportion of RE generation, the MBSO algorithm achieves 98.65%, higher than the BSO algorithm's 97.56%. This indicates that the MBSO algorithm is more effective in increasing the proportion of RE in the total power generation, which helps to promote the green transformation of the energy structure. In terms of satisfaction score, the MBSO algorithm scored 1.89, which is higher than the BSO algorithm's score of 1.45. This indicates that the BSO algorithm has shortcomings in improving user satisfaction and is difficult to fully meet user needs. In contrast, the MBSO algorithm more effectively improved user satisfaction and brought significant economic and social benefits to the power system. In terms of RE generation utilization, the MBSO algorithm achieves 100%, significantly higher than the BSO algorithm's 88.79%. The MBSO algorithm can better utilize RE, reduce energy waste, and improve energy utilization efficiency.

3. Results and Discussion

3.1 Ablation Analysis of The Modified Components

To verify the individual contributions of the two modified components in MBSO, three variants are constructed: BSO without any modification, MBSO-NS with only the non-dominated sorting mechanism, and MBSO with both non-dominated sorting and crowding degree computing mechanisms. The results show that MBSO-NS already reduces the variance and standard deviation compared with BSO on all three benchmark functions, while MBSO further reduces these statistical measures and improves the optimal values on the Step and Rastrigin functions. In the power grid scheduling application, MBSO-NS improves the VQ from 0.37 to 0.39 and the REUR from 88.79% to 93.46%, while MBSO further raises them to 0.41 and 100%. These results confirm that both modified components contribute individually to the performance improvement, and their combination produces the best overall performance.

3.2 Statistical Comparison with Other Optimization Algorithms

The MBSO algorithm is compared with BSO, PSO and GA under identical population size, iteration number, stopping criteria and 30 independent runs. On the test set of NSL-KDD, the average fitness values of MBSO, BSO, PSO and GA are 0.10, 0.22, 0.28 and 0.31, respectively, with MBSO showing the smallest standard deviation. The p-values of MBSO versus PSO and MBSO versus GA are 0.009 and 0.004, both below 0.05, indicating that the advantages of MBSO are statistically significant. Compared with GA, MBSO handles multi-objective optimization more effectively by avoiding the dispersion of solution sets; compared with PSO, MBSO reduces the impact of randomness and achieves higher stability and convergence speed.

3.3 Discussion on VQ and RE Utilization

The four performance indices are calculated according to the definitions given in Section 2.3. In terms of VQ, MBSO scores 0.41, higher than the 0.37 of BSO, indicating that the node voltages are closer to the rated value. In terms of REGR, MBSO achieves 98.65%, higher than the 97.56% of BSO, confirming a larger share of clean energy in the power supply structure. In terms of SV, MBSO scores 1.89, higher than the 1.45 of BSO. In terms of renewable energy generation utilization ratio, MBSO achieves 100%, significantly higher than the 88.79% of BSO, which means that all available RE is fully consumed under MBSO-based scheduling while 11.21% is curtailed under BSO-based scheduling.

3.4 Limitations and Practical Applicability

The proposed method has several limitations. It is validated only on the IEEE 35-node ADS with data from a specific region in northwest China, so its applicability to other network topologies and larger-scale systems needs further verification. The model does not fully incorporate demand-side peak shaving and valley filling measures, which may limit its application in markets with strong

demand-side response requirements. The computational time of MBSO is slightly longer than that of BSO, and some parameters still rely on empirical selection. In terms of practical applicability, the method can be directly applied to ADSs with high penetration of wind and photovoltaic generation, providing operators with a quantitative scheduling scheme on a 15-minute resolution over a 24-hour horizon. The Pareto solution set allows operators to select the most suitable plan according to different preferences, and the method can be integrated into existing distribution management systems without additional hardware investment.

4. Conclusions

For the optimization of power generation systems with efficient use of RE sources, this study established a COSM for REGS by improving the updating method of BSO and adopting the combination of MBSO and ADS. The main conclusions are as follows. First, the MBSO algorithm achieved better optimization performance than the traditional BSO algorithm. The optimal values of MBSO for the Sphere, Step, and Rastrigin functions were 0.0132, 0.0119, and 0.0657, respectively, with mean ± variance values of 0.0276 ± 0.0183, 0.0185 ± 0.0164, and 0.0644 ± 0.0143, which were all improved compared to BSO, and the variances were significantly lower, indicating higher optimization accuracy and stability. Second, the ablation analysis confirmed the individual contribution of the modified components. MBSO-NS improved the VQ from 0.37 to 0.39 and the renewable energy utilization ratio from 88.79% to 93.46%, while MBSO further raised them to 0.41 and 100%, demonstrating that both non-dominated sorting and crowding degree computing mechanisms contribute individually and their combination produces the best performance. Third, the statistical comparison confirmed the robustness of the proposed method. The average fitness values of MBSO, BSO, PSO, and GA on the test set were 0.10, 0.22, 0.28, and 0.31, respectively, with MBSO showing the smallest standard deviation, and the p-values of MBSO versus PSO and MBSO versus GA were 0.009 and 0.004, both below 0.05, indicating statistically significant advantages. Fourth, the power grid simulation verified the effectiveness of the proposed method. The voltage prediction error was within 0 to 0.003, the node voltages after optimal dispatch remained between 0.93 p.u. and 1.07 p.u., the VQ increased to 0.41, the share of RE generation and usage efficiency increased by 1.09% and 11.21%, respectively, and the SV increased from 1.45 to 1.89. Finally, the limitations and practical applicability were clarified. The method was validated only on the IEEE 35-node system with data from northwest China, and its extension to other topologies, demand-side response measures, and adaptive parameter tuning requires further research. Nevertheless, the method can be directly applied to ADSs with high penetration of RE, providing operators with a quantitative scheduling scheme and a Pareto solution set for selecting the most suitable plan without additional hardware investment.

Fundings

The research is supported by the Research on Key Technologies of Multi-Resource Aggregation and Simulation for Virtual Power Plants, Research Funding Project for Introduced Talents of Taiyuan Institute of Technology .(No.2025KJ001)

References

[1] Nepal R, Musibau HO. Energy security, renewable, non-renewable energy and economic growth in ASEAN economies: new insights. The Singapore Economic Review. 2021;66(02):457-488. https://doi.org/10.1142/S0217590819430045

[2] Guo P, Sun F, Han X. Study on comprehensive evaluation of environmental pollution treatment effect in coal mine subsidence area: taking Xinglongzhuang mining area of Yanzhou energy as an example. Environmental Science and Pollution Research. 2023;30(3):6132-6145. https://doi.org/10.1007/s11356-022-22532-9

[3] Usman AM, Abdullah MK. An assessment of building energy consumption characteristics using analytical energy and carbon footprint assessment model. Green and Low-Carbon Economy. 2023;1(1):28-40. https://doi.org/10.47852/bonviewGLCE3202545

[4] Song L, Tian K, Jiao X, Feng R, Wang L, Tian R. Design and optimization of seagull airfoil wind energy conversion device. International Journal of Green Energy. 2021;18(10):1046-1063. https://doi.org/10.1080/15435075.2021.1890087

[5] Meenal R, Binu D, Ramya KC, Vinoth Kumar K, Rajasekaran E, Sangeetha B. Weather forecasting for renewable energy system: a review. Archives of Computational Methods in Engineering. 2022;29(5):2875-2891. https://doi.org/10.1007/s11831-021-09695-3
[6] Blaabjerg F, Yang Y, Kim KA, Rodriguez J. Power electronics technology for large-scale renewable energy generation. Proceedings of the IEEE. 2023;111(4):335-355. https://doi.org/10.1109/JPROC.2023.3253165
[7] Murphy LR, Daly SR, Seifert CM. Idea characteristics arising from individual brainstorming and design heuristics ideation methods. International Journal of Technology and Design Education. 2023;33(2):337-378. https://doi.org/10.1007/s10798-021-09723-0
[8] Kumar L, Gupta SK, Kumar S. A novel brainstorm-based optimization method for optimum planning of reactive power with FACTS devices. International Journal of System Assurance Engineering and Management. 2022;13(6):3062-3073. https://doi.org/10.1007/s13198-022-01802-2
[9] Alzaqebah M, Jawarneh S, Alwohaibi M, Alsmadi MK, Almarashdeh I, Mohammad RMA. Hybrid brain storm optimization algorithm and late acceptance hill climbing to solve the flexible job-shop scheduling problem. Journal of King Saud University-Computer and Information Sciences. 2022;34(6):2926-2937. https://doi.org/10.1016/j.jksuci.2020.09.004
[10] Zheng J, Lin Z, Xie X. Improved multi-objective brain storm optimization algorithm for RFID network planning. Wireless Networks. 2024;30(2):1055-1068. https://doi.org/10.1007/s11276-023-03543-x
[11] Guo X, Shang F, Chen J. Software running defect recognition method based on brainstorming optimisation algorithm. International Journal of Reasoning-based Intelligent Systems. 2024;16(2):137-146. https://doi.org/10.1504/IJRIS.2024.138622
[12] Alwohaibi M, Alzaqebah M, Alotaibi NM, Alzahrani AM, Zouch M. A hybrid multi-stage learning technique based on brain storming optimization algorithm for breast cancer recurrence prediction. Journal of King Saud University-Computer and Information Sciences. 2022;34(8):5192-5203. https://doi.org/10.1016/j.jksuci.2021.05.004
[13] Lavrič F, Škraba A. Brainstorming will never be the same again-A human group supported by artificial intelligence. Machine Learning and Knowledge Extraction. 2023;5(4):1282-1301. https://doi.org/10.3390/make5040065
[14] Raamesh L, Jothi S, Radhika S. Enhancing software reliability and fault detection using hybrid brainstorm optimization-based LSTM model. IETE Journal of Research. 2023;69(12):8789-8803. https://doi.org/10.1080/03772063.2022.2069603
[15] Zheng W, Lu H, Zhang M, Wu Q, Hou Y, Zhu J. Distributed energy management of multi-entity integrated electricity and heat systems: A review of architectures, optimization algorithms, and prospects. IEEE Transactions on Smart Grid. 2023;15(2):1544-1561. https://doi.org/10.1109/TSG.2023.3310947
[16] Liu LN, Yang GH. Distributed optimal energy management for integrated energy systems. IEEE Transactions on Industrial Informatics. 2022;18(10):6569-6580. https://doi.org/10.1109/TII.2022.3146165
[17] Makahleh FM, Amer A, Manasrah AA, Attar H, Solyman AAA, Kamarposhti MA, Thounthong P. Optimal management of energy storage systems for peak shaving in a smart grid. Computers, Materials and Continua. 2023;75(2):3317-3337. https://doi.org/10.32604/cmc.2023.035690
[18] Habib S, Kamarposhti MA, Shokouhandeh H, Colak I, Manaa Barhoumi EL. Economic dispatch optimization considering operation cost and environmental constraints using the HBMO method. Energy Reports. 2023;10:1718-1725. https://doi.org/10.1016/j.egyr.2023.08.032
[19] Kamarposhti MA, Colak I, Shokouhandeh H, Iwendi C, Padmanaban S, Band SS. Optimum operation management of microgrids with cost and environment pollution reduction approach considering uncertainty using multi-objective NSGAII algorithm. IET Renewable Power Generation. 2025;19(1):e12579. https://doi.org/10.1049/rpg2.12579
[20] Shokouhandeh H, Ahmadi Kamarposhti M, Asghari F, Colak, Eguchi K. Distributed generation management in smart grid with the participation of electric vehicles with respect to the vehicle owners' opinion by using the imperialist competitive algorithm. Sustainability. 2022;14(8):4770. https://doi.org/10.3390/su14084770
[21] Li H, Hao T, Li Z, Zhao E, Wang C, Xu L. Research on a self-coordinated optimization method for distributed energy resources targeting risk mitigation. Distributed Generation and Alternative Energy Journal. 2024;39(3):659-690. https://doi.org/10.13052/dgaej2156-3306.39312
[22] Hiremath R, Moger T. Improving the DC-link voltage of DFIG driven wind system using modified sliding mode control. Distributed Generation and Alternative Energy Journal. 2023;38(3):715-742. https://doi.org/10.13052/dgaej2156-3306.3831
[23] Sundarajoo S, Soomro DM. Artificial neural network-based voltage stability online monitoring approach for distributed generation integrated distribution system. Distributed Generation and Alternative Energy Journal. 2023;38(06):1839-1862. https://doi.org/10.13052/dgaej2156-3306.3866

[24] Kumari P, Sahana SK. PSO-DQ: An improved routing protocol based on PSO using dynamic queue mechanism for MANETs. Journal of Information Science & Engineering. 2022;38(1):41-56.
[25] Ghiduk AS, Alharbi A. Generating of test data by harmony search against genetic algorithms. Intelligent Automation & Soft Computing. 2023;36(1):647-665. https://doi.org/10.32604/iasc.2023.031865